Mechanism and Machine Theory 130 (2018) 363–381

Contents lists available at ScienceDirect

Mechanism and Machine Theory

journal homepage: www.elsevier.com/locate/mechmachtheory

Research paper

Dynamic driveline torque estimation during whole gear shift for an automatic transmission

Hyunseok Choi[a], Jaewoong Hwang[b], Seibum Choi[a,*]

[a] Department of Mechanical Engineering, KAIST, 291 Daehak-ro Yuseong-gu, Daejeon 34141, Republic of Korea
[b] The 5th Research & Development Institute, Agency for Defense Development, Yuseong P.O.Box 35, Daejeon 34186, Republic of Korea

ARTICLE INFO

Article history:
Received 11 May 2018
Revised 23 July 2018
Accepted 24 August 2018
Available online 12 September 2018

Keywords:
Automatic transmission
Clutch-to-clutch shift
Clutch torque estimation
Drive shaft torque estimation
Gear shift control

ABSTRACT

This study proposes a novel method for estimation of driveline torque of wet type AT (Automatic transmission). The previous methods of torque estimation in the clutch-to-clutch shift mechanism is mainly applicable to the single gear shift. Thus, they require specific definitions of each gear shift and signal processing corresponding to the multi-gear shift. This study distinctly develops driveline torque estimator based on the whole transmission model, which is capable in applying on any conditional gear shift. This paper, also, incomparably investigates brake/clutch model including centrifugal force, describing physical behavior of real parts. In addition, the development of the method includes adaptive brake and clutch torque estimator in order to compensate variation factor during the shift. The estimation performance of the proposed estimator is evaluated both in simulations and experiments. The results demonstrate that the proposed methods can estimate the driveline torques effectively during the whole gear shift and well describes the typical clutch-to-clutch phenomena such as inter-locking.

1. Introduction

Automatic transmission (AT) bridges power from engine to drive wheel with the automatic shift strategies. It is capable in drawing immense torque increase and exceptional shift quality with the help of torque converter and multiple planetary gears. As a result, AT has been widely adopted in vehicle industries including passenger and commercial vehicles; however, various transmission types that lacks torque converter such as Dual Clutch Transmission (DCT) or Continuously Variable Transmission (CVT) has been introduced for fulfilling customers' expectation for vehicles to be compact and fuel efficient. In fact, as the powertrain downsizing has become one of the critical issues in order to maximize the vehicle performance, the mechanical structure of AT has been modified for compact size, resulting in satisfactory fuel efficiency and shift quality. As a result, the size issue of AT due to the existence of torque converter has been resolved from exchanging the complex and bulky one-way clutches to friction clutches and adopting newly introduced clutch-to-clutch shift. Such shift skim is similar to that of DCT except that torque converter is exploited for vast torque increase at the vehicle launching stage [1,2]. Since usage of torque converter is limited in the earlier shift stage, precise shift control strategy now became a critical factor in guaranteeing exceptional shift quality with minimization of shift impact. Among various control strategies, speed-based control [3,4] was widely adopted; however, the limitation of such control method yields difficulty in using speed feedback during torque phase [5]. Therefore, torque feedback control strategy alternatively has been adopted to acquire an

* Corresponding author.
E-mail address: sbchoi@kaist.ac.kr (S. Choi).

https://doi.org/10.1016/j.mechmachtheory.2018.08.024
0094-114X/

extraordinary shift performance due to the simplicity of utilizing torque from engine to the wheel axle. Thus, torque-base control strategies, which are applicable to DCT, for improving shift quality has become the leading research area for vehicle transmission shift control [6–11].

The transmission size constraints and cost issues from implementing torque sensors to each clutch and drive shaft inevitably cause difficulty in applying torque-base control algorithm. In order to overcome such hampers, numerous researches have suggested drive shaft torque estimation methods without torque sensors [12–14]. Several estimation methods include the nonlinear sliding mode observers [15,16] and two different methods for estimating the drive shaft torque by employing the characteristics of the engine torque map and turbine torque map [17]. In fact, such methods fit for the estimation process of the drive shaft torque of Automated Manual Transmissions (AMTs) [18,19]. However, suggested torque estimation methods are unsuitable in applying for clutch-to-clutch shift since two clutches operates simultaneously in achieving a shift. Another research proposes the torque estimation methods for DCT driveline for the case of vehicle launch where only one clutch operates [20–23]. Some research, also, suggests the application of such estimation method for two clutches simultaneously operating in earlier launch phase from utilizing high-order sliding mode observer [24].

The clutch torque estimation for the clutch-to-clutch shift is more challenging than that of one-clutch engagement such as AMT due to the fact that both clutches concurrently operates, which makes the system over-actuated. The previous study analyzes the relation of speed and torque during clutch-to-clutch shift [25]. In fact, several recent researches for clutch-to-clutch shift have been proposed including torque estimation using unscented Kalman filters [26,27]: joint extended Kalman filter and dual extended Kalman filter [28], Takagi-Sugeno observer [29]. Such clutch-to-clutch shift method, however, overlook concurrent operation of clutches. In fact, other researchers suggest novel torque estimators from combining multiple observers in case of clutch to clutch concurrent gear shifts for DCT [30,31]; however, torque estimation method from combining multiple observer increases implementation complexity. To overcome this problem, other researches have suggested torque estimator using respective reduced order mode according to the shift phases (torque phase and inertia phase) for DCT with practical concerns [32,33]. In fact, other researches have suggested nonlinear sliding mode observer for AT according to the shift phases [34]. Although, this method handles the clutch-to-clutch shifts of AT with planetary gears, it's modelling is based on single shift like DCT.

The limitation of previously suggested torque estimation methods becomes apparent in the case of multiple gear shifts as they are mainly developed for single gear shift. The application of such methods to the real multi-step transmission requires additional formulations to calculate each gear ratio. Such work is more complex for AT than for DCT as AT uses many planetary gears together, while DCT uses only spur gears. Furthermore, additional signal processing is needed as the switching from one shift to other shift makes frequent jumps of estimators [31]. In order to overcome these issues, this research distinctly develops the whole transmission model for AT, which is capable in applying on any conditional gear shifts. This research, also, incomparably investigates brake/clutch model including centrifugal force, closely describing the physical behavior of real parts. In addition, the proposed method is also robust in torque estimation with the presence of parametric errors such as variation of the clutch parameters. In fact, with relatively simple implementation process, the estimation performance of shaft speed and clutch/brake torque are exceptional. The proposed state estimator is verified by applying to a specific tracked vehicle transmission; furthermore, such estimator is also capable in applying for other or simpler types of AT as well.

The rest of this paper is organized as follows: Section two introduces the transmission model of the six-speed tracked vehicle transmission and the design process of the torque estimator upon the model. Section three proposes the effectiveness of the state estimator, which is demonstrated via the simulation. Section four summarizes and discusses about the experiment method and result of the proposed estimator in depth. Section five, concludes the paper.

2. Dynamic torque estimation strategy

2.1. Transmission overview

The transmission studied in this paper is a wet type six-speed automatic transmission for tracked vehicles. Fig. 1 illustrates the clutch-pack which is consisted of two major parts. The first part consists three planetary gears (P4, PF, and PR) and two brakes (BF and BR) for controlling the driving direction of vehicle (forward and reverse). The second part composes three planetary gears (P1, P2 and P3), three brakes (B1, B2, B3), and two clutches (C1 and C2) for controlling the shift range from 1st to 6th gear. Table 1 shows the combination of engaged brakes and clutches in each gear for corresponding gear. Brake engagement in the first part and engagement of clutch/brakes in the second part realizes six-speed ranges for forward and reverse direction. For reverse direction, 4th, 5th and 6th gears are automatically restricted by transmission control unit (TCU) for driving safety.

2.2. Dynamic gear shift modeling

Since the gear shift operates only in the second part, the paper only investigates mathematical modeling of the second part. Fig. 2 illustrates the free-body diagram of the second part. Here T, I, R_r, F, ω, S and R mean torque, inertia, driving resistance, internal force or torque, speed, the radii of sun gear and ring gear respectively. The subscriptions *i, o, r, c* and *s*

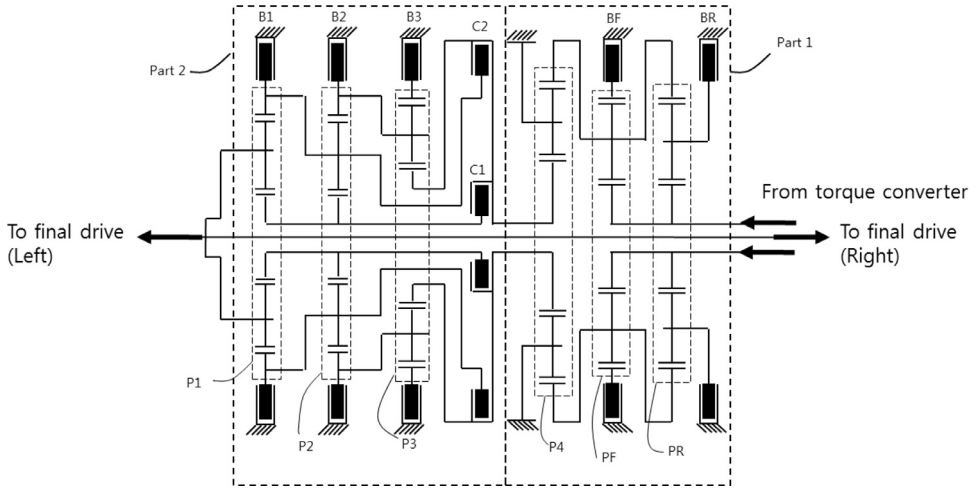

Fig. 1. Schematic diagram of the six-speed clutch-pack for tracked vehicle.

Table 1
Engaged brakes and clutches on each gear.

Direction/ gear		Engaged brakes and clutches						
		BF	BR	B1	B2	B3	C1	C2
Forward	1st	○		○			○	
	2nd	○			○		○	
	3rd	○				○	○	
	4th	○					○	○
	5th	○				○		○
	6th	○			○			○
Reverse	1st		○	○			○	
	2nd		○		○		○	
	3rd		○			○	○	

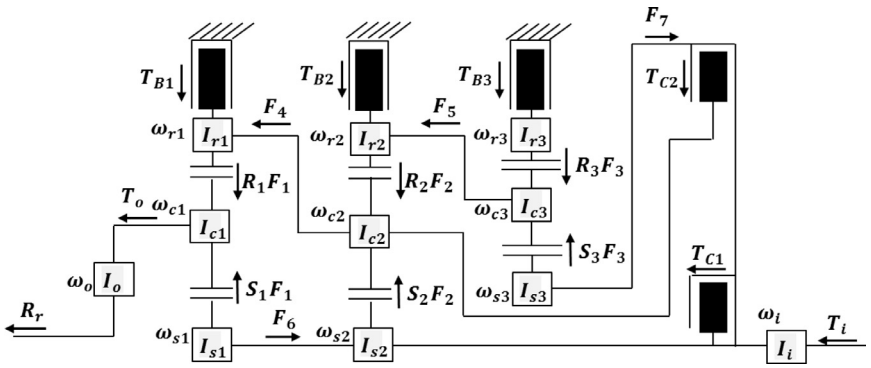

Fig. 2. Free body diagram of the second part.

mean input shaft, output shaft, ring gear, carrier and sun gear respectively. The whole gear shift modeling procedure using Lagrange equation is similar to that of reference [35].

Driving resistance is expressed in Eq. (1).

$$R_r = \left(f_r Mgcos(\theta) + Mgsin(\theta) + \frac{1}{2}\rho_a A C_D v^2\right) r_s / N_{FD}, \tag{1}$$

where f_r, M, g, θ, ρ_a, A, C_D, v, r_s and N_{FD} state the coefficient of rolling resistance, vehicle mass, gravity acceleration, road slope, density of air, frontal area of the vehicle, drag coefficient, vehicle speed, sprocket radius and gear ratio of final drive respectively.

Eleven differential equations can be drawn from the relationships of the sun, carrier and ring gear dynamics in each planetary gear and input and output shaft as shown in equations (2) ~ (12).

$$I_i\dot{\omega}_i = T_i + F_7 - T_{c1} - T_{c2}, \tag{2}$$

$$I_o\dot{\omega}_o = T_o - R_r, \tag{3}$$

$$I_{s1}\dot{\omega}_{s1} = -S_1F_7 - F_6, \tag{4}$$

$$I_{r1}\dot{\omega}_{r1} = F_4 + T_{B1} - R_1F_1, \tag{5}$$

$$I_{c1}\dot{\omega}_{c1} = (S_1 + R_1)F_1 - T_o, \tag{6}$$

$$I_{s2}\dot{\omega}_{s2} = T_{C1} - S_2F_2 + F_6, \tag{7}$$

$$I_{r2}\dot{\omega}_{r2} = F_5 + T_{B2} - R_2F_2, \tag{8}$$

$$I_{c2}\dot{\omega}_{c2} = T_{C2} + (S_2 + R_2)F_2 - F_4, \tag{9}$$

$$I_{s3}\dot{\omega}_{s3} = -S_3F_3 - F_7, \tag{10}$$

$$I_{r3}\dot{\omega}_{r3} = T_{B3} - R_3F_3, \tag{11}$$

$$I_{c3}\dot{\omega}_{c3} = (S_3 + R_3)F_3 - F_5. \tag{12}$$

In addition, eight speed constraints equations are constituted by three planetary speed constraints and five speed connections as shown in Eqs. (13) ~ (20).

$$\omega_{s1}S_1 + \omega_{r1}R_1 = \omega_{c1}(S_1 + R_1), \tag{13}$$

$$\omega_{s2}S_2 + \omega_{r2}R_2 = \omega_{c2}(S_2 + R_2), \tag{14}$$

$$\omega_{s3}S_3 + \omega_{r3}R_3 = \omega_{c3}(S_3 + R_3), \tag{15}$$

$$\omega_{r1} = \omega_{c2}, \tag{16}$$

$$\omega_{r2} = \omega_{c3}, \tag{17}$$

$$\omega_{s1} = \omega_{s2}, \tag{18}$$

$$\omega_i = \omega_{s3}, \tag{19}$$

$$\omega_o = \omega_{c1}. \tag{20}$$

By assigning the unknown variable which are speeds, internal force/torque and output shaft torque to the left side and the known (or assumed to be known) variables which are torques of input shaft and brake and clutch and driving resistance to the right side, matrix format can be constituted as shown in Eq. (21). Eqs. (22) and (23) shows the details of such matrix. The M is 19 by 19 matrix and it is invertible. So it is possible to solve the unknown variables uniquely by Eq. (24).

$$\mathrm{M}\Omega = BT, \tag{21}$$

$$M = \begin{bmatrix}
I_{s1} & 0 & 0 & 0 & 0 & 0 & 0 & 0 & 0 & 0 & 0 & S_1 & 0 & 0 & 0 & 0 & 1 & 0 & 0 \\
0 & I_{r1} & 0 & 0 & 0 & 0 & 0 & 0 & 0 & 0 & 0 & R_1 & 0 & 0 & -1 & 0 & 0 & 0 & 0 \\
0 & 0 & I_{c1} & 0 & 0 & 0 & 0 & 0 & 0 & 0 & 0 & -(S_1+R_1) & 0 & 0 & 0 & 0 & 0 & 0 & 1 \\
0 & 0 & 0 & I_{s2} & 0 & 0 & 0 & 0 & 0 & 0 & 0 & 0 & S_2 & 0 & 0 & 0 & -1 & 0 & 0 \\
0 & 0 & 0 & 0 & I_{r2} & 0 & 0 & 0 & 0 & 0 & 0 & 0 & R_2 & 0 & 0 & -1 & 0 & 0 & 0 \\
0 & 0 & 0 & 0 & 0 & I_{c2} & 0 & 0 & 0 & 0 & 0 & -(S_2+R_2) & 0 & 1 & 0 & 0 & 0 & 0 & 0 \\
0 & 0 & 0 & 0 & 0 & 0 & I_{s3} & 0 & 0 & 0 & 0 & 0 & S_3 & 0 & 0 & 0 & 1 & 0 & 0 \\
0 & 0 & 0 & 0 & 0 & 0 & 0 & I_{r3} & 0 & 0 & 0 & 0 & R_3 & 0 & 0 & 0 & 0 & 0 & 0 \\
0 & 0 & 0 & 0 & 0 & 0 & 0 & 0 & I_{c3} & 0 & 0 & 0 & -(S_3+R_3) & 0 & 1 & 0 & 0 & 0 & 0 \\
0 & 0 & 0 & 0 & 0 & 0 & 0 & 0 & 0 & I_i & 0 & 0 & 0 & 0 & 0 & 0 & -1 & 0 & 0 \\
0 & 0 & 0 & 0 & 0 & 0 & 0 & 0 & 0 & 0 & I_o & 0 & 0 & 0 & 0 & 0 & 0 & -1 & 0 \\
S_1 & R_1 & -(S_1+R_1) & 0 & 0 & 0 & 0 & 0 & 0 & 0 & 0 & 0 & 0 & 0 & 0 & 0 & 0 & 0 & 0 \\
0 & 0 & 0 & S_2 & R_2 & -(S_2+R_2) & 0 & 0 & 0 & 0 & 0 & 0 & 0 & 0 & 0 & 0 & 0 & 0 & 0 \\
0 & 0 & 0 & 0 & 0 & 0 & S_3 & R_3 & -(S_3+R_3) & 0 & 0 & 0 & 0 & 0 & 0 & 0 & 0 & 0 & 0 \\
0 & -1 & 0 & 0 & 0 & 1 & 0 & 0 & 0 & 0 & 0 & 0 & 0 & 0 & 0 & 0 & 0 & 0 & 0 \\
0 & 0 & 0 & 0 & -1 & 0 & 0 & 0 & 1 & 0 & 0 & 0 & 0 & 0 & 0 & 0 & 0 & 0 & 0 \\
1 & 0 & 0 & -1 & 0 & 0 & 0 & 0 & 0 & 0 & 0 & 0 & 0 & 0 & 0 & 0 & 0 & 0 & 0 \\
0 & 0 & 0 & 0 & 0 & 0 & 1 & 0 & 0 & -1 & 0 & 0 & 0 & 0 & 0 & 0 & 0 & 0 & 0 \\
0 & 0 & 1 & 0 & 0 & 0 & 0 & 0 & 0 & 0 & -1 & 0 & 0 & 0 & 0 & 0 & 0 & 0 & 0
\end{bmatrix},$$

$$\Omega = \begin{bmatrix}
\dot{\omega}_{s1} \\ \dot{\omega}_{r1} \\ \dot{\omega}_{c1} \\ \dot{\omega}_{s2} \\ \dot{\omega}_{r2} \\ \dot{\omega}_{c2} \\ \dot{\omega}_{s3} \\ \dot{\omega}_{r3} \\ \dot{\omega}_{c3} \\ \dot{\omega}_i \\ \dot{\omega}_o \\ F_1 \\ F_2 \\ F_3 \\ F_4 \\ F_5 \\ F_6 \\ F_7 \\ T_o
\end{bmatrix}, \tag{22}$$

$$\mathrm{B} = \begin{bmatrix}
0 & 0 & 0 & 0 & 0 & 0 & 0 \\
1 & 0 & 0 & 0 & 0 & 0 & 0 \\
0 & 0 & 0 & 0 & 0 & 0 & 0 \\
0 & 0 & 0 & 1 & 0 & 0 & 0 \\
0 & 1 & 0 & 0 & 0 & 0 & 0 \\
0 & 0 & 0 & 0 & 1 & 0 & 0 \\
0 & 0 & 0 & 0 & 0 & 0 & 0 \\
0 & 0 & 1 & 0 & 0 & 0 & 0 \\
0 & 0 & 0 & 0 & 0 & 0 & 0 \\
0 & 0 & 0 & -1 & -1 & 1 & 0 \\
0 & 0 & 0 & 0 & 0 & 0 & -1 \\
0 & 0 & 0 & 0 & 0 & 0 & 0 \\
0 & 0 & 0 & 0 & 0 & 0 & 0 \\
0 & 0 & 0 & 0 & 0 & 0 & 0 \\
0 & 0 & 0 & 0 & 0 & 0 & 0 \\
0 & 0 & 0 & 0 & 0 & 0 & 0 \\
0 & 0 & 0 & 0 & 0 & 0 & 0 \\
0 & 0 & 0 & 0 & 0 & 0 & 0 \\
0 & 0 & 0 & 0 & 0 & 0 & 0
\end{bmatrix}, \quad \mathrm{T} = \begin{bmatrix}
\mathrm{T}_{B1} \\ \mathrm{T}_{B2} \\ \mathrm{T}_{B3} \\ \mathrm{T}_{C1} \\ \mathrm{T}_{C2} \\ \mathrm{T}_i \\ R_r
\end{bmatrix}, \tag{23}$$

$$\Omega = M^{-1}BT. \tag{24}$$

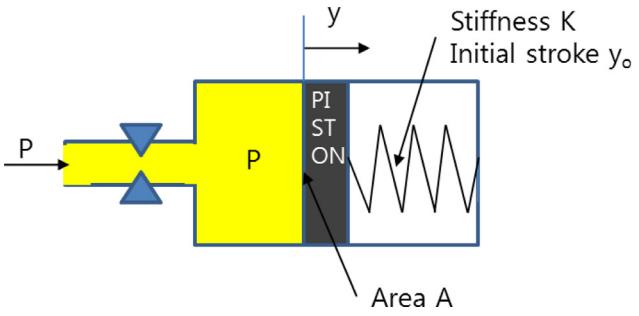

Fig. 3. Brake cross-section diagram.

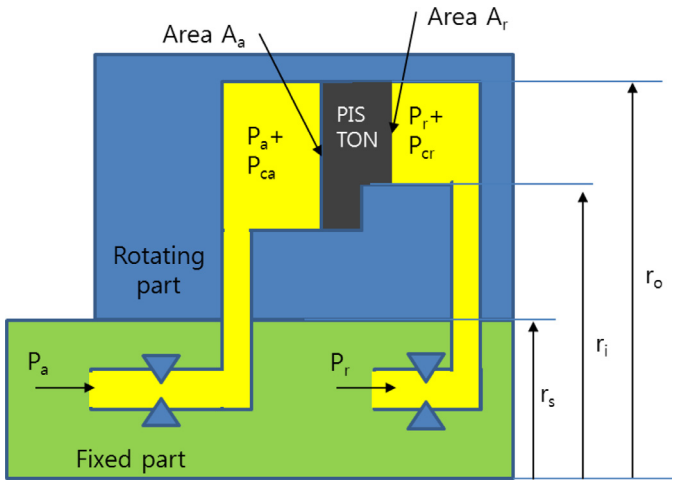

Fig. 4. Clutch cross-section diagram.

2.3. Brake and clutch torque calculation

In the T matrix, input shaft torque T_i is measured by an engine sensor. Driving resistance R_r is calculated in Eq. (1), which is assumed to be known. Note that, alternatively, it can be calculated from stiffness, damping coefficient, and the difference between transmission output shaft and wheel displacement with the information of wheel speed sensors; however, typical tracked vehicles lack wheel speed sensors.

Building process for friction forces requires classification between brake and clutch. This is because purposes of brakes and clutches differ: brake stops the rolling part whereas clutch synchronizes two rolling parts from different speeds into a same speed. As a result, the mechanical structure of brake piston includes return spring since brakes are not designed for consistent rotation. On the other hand, as a clutch is designed for constant rotation throughout the process, simple implementation of return spring is not desirable due to structural difficulty. Thus, the necessary return force for clutch piston is produced throughout return pressure in the clutch. Thus, distinct modeling for each component type is inevitable in order to describe mechanical behavior of the real brake and clutch.

Typically, hyperbolic functions are suitable for representing clutch/brake friction behavior modeling due to its continuous characteristics. The main purpose of using one continuous hyperbolic function is to avoid discontinuity problem from modeling three different equations corresponding to each clutch/brake state transition. Fig. 3 shows cross-section diagram of the brake (the diagram itself lacks friction plates for simplicity) where resulting brake torque can be modeled as Eq. (25).

$$T_B = \mu n r(A \cdot p - K(y_o + y))tanh(\Delta\omega/\alpha) \tag{25}$$

where μ, n, r, A, p, K, y_o and α mean brake/clutch friction coefficient, number of friction side, effective radius of clutch, piston area, piston pressure, spring stiffness, initial pressed length of return spring and tuning parameter respectively. Each brake pressure is monitored using a pressure sensor.

Piston stroke can be calculated by Eq. (26) where, γ is a damping coefficient of the transmission oil

$$M\ddot{y} = A \cdot p - K(y_o + y) - \gamma\dot{y}. \tag{26}$$

Fig. 4 shows clutch cross-section diagram (the diagram itself lacks friction plates for simplicity). For clutch torque calculation, centrifugal pressure should be considered because piston oil is rotating. Eq. (27) shows the clutch torque calculation where the subscriptions *a, ca, r* and *cr* are action piston, centrifugal effect on action piston, return piston and centrifugal

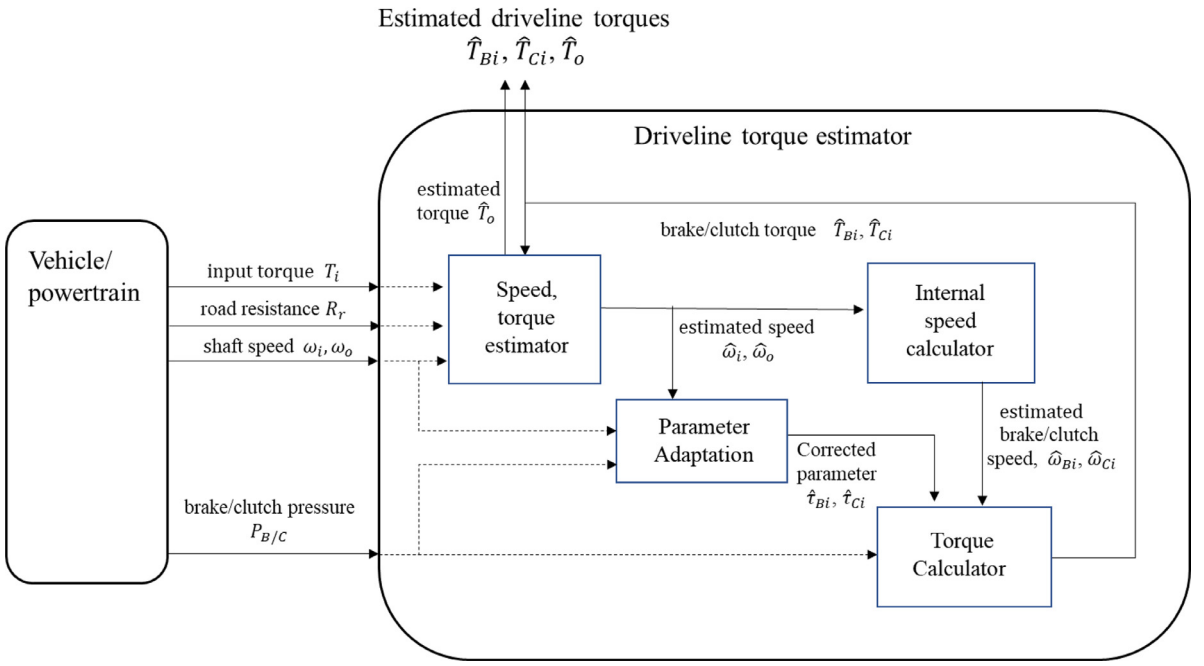

Fig. 5. Torque estimator structure.

effect on return piston respectively.

$$T_C = \mu nr\{A_a(p_a + p_{ca}) - A_r(p_r + p_{cr})\}tanh(\Delta\omega/\alpha). \tag{27}$$

Centrifugal pressure is calculated as shown in Eq. (28) where, ρ_o represents density of transmission oil.

$$P_c = \frac{\rho_o \omega^2}{2}\left(\frac{{r_o}^2 + {r_i}^2}{2} - {r_s}^2\right). \tag{28}$$

Therefore, all the brake and clutch torques can be calculated if slip speeds are informed.

2.4. Internal planetary gear speed calculation

Now, brake/clutch slip speed needs to be calculated from tangent hyperbolic function. In order to calculate the brake/clutch slip speed, internal planetary gear speed needs to be known which can be calculated from the input and output speed. Since there are eleven speed variables, eight speed constraints, and two equations from the input/output speed measurements, one more equation is required to yield the unique solution, which can be formed from one closed clutch relation. During 1st to 4th gear, C1 clutch is closed which means input speed is identical to second sun-gear speed. During 4th to 6th gear, C2 clutch is closed which means input speed is identical to second carrier speed. Eq. (29) shows the clutch speed matrix. Therefore, a unique solution can be obtained.

$$\begin{bmatrix} S_1 & R_1 & -(S_1+R_1) & 0 & 0 & 0 & 0 & 0 & 0 & 0 & 0 \\ 0 & 0 & 0 & S_2 & R_2 & -(S_2+R_2) & 0 & 0 & 0 & 0 & 0 \\ 0 & 0 & 0 & 0 & 0 & 0 & S_3 & R_3 & -(S_3+R_3) & 0 & 0 \\ 0 & -1 & 0 & 0 & 0 & 1 & 0 & 0 & 0 & 0 & 0 \\ 0 & 0 & 0 & 0 & -1 & 0 & 0 & 0 & 1 & 0 & 0 \\ 1 & 0 & 0 & -1 & 0 & 0 & 0 & 0 & 0 & 0 & 0 \\ 0 & 0 & 0 & 0 & 0 & 0 & 1 & 0 & 0 & -1 & 0 \\ 0 & 0 & 1 & 0 & 0 & 0 & 0 & 0 & 0 & 0 & -1 \\ 0 & 0 & 0 & a & 0 & b & 0 & 0 & 0 & 1 & 0 \\ 0 & 0 & 0 & 0 & 0 & 0 & 0 & 0 & 0 & 1 & 0 \\ 0 & 0 & 0 & 0 & 0 & 0 & 0 & 0 & 0 & 0 & 1 \end{bmatrix} \begin{bmatrix} \omega_{s1} \\ \omega_{r1} \\ \omega_{c1} \\ \omega_{s2} \\ \omega_{r2} \\ \omega_{c2} \\ \omega_{s3} \\ \omega_{r3} \\ \omega_{c3} \\ \omega_i \\ \omega_o \end{bmatrix} = \begin{bmatrix} 0 & 0 \\ 0 & 0 \\ 0 & 0 \\ 0 & 0 \\ 0 & 0 \\ 0 & 0 \\ 0 & 0 \\ 0 & 0 \\ 0 & 0 \\ 1 & 0 \\ 0 & 1 \end{bmatrix} \begin{bmatrix} \omega_i \\ \omega_o \end{bmatrix}, \tag{29}$$

which summarizes the discussion where $a = -1,\ b = 0$ during 1st to 4th gear and $a = 0,\ b = -1$ during 4th to 6th gear.

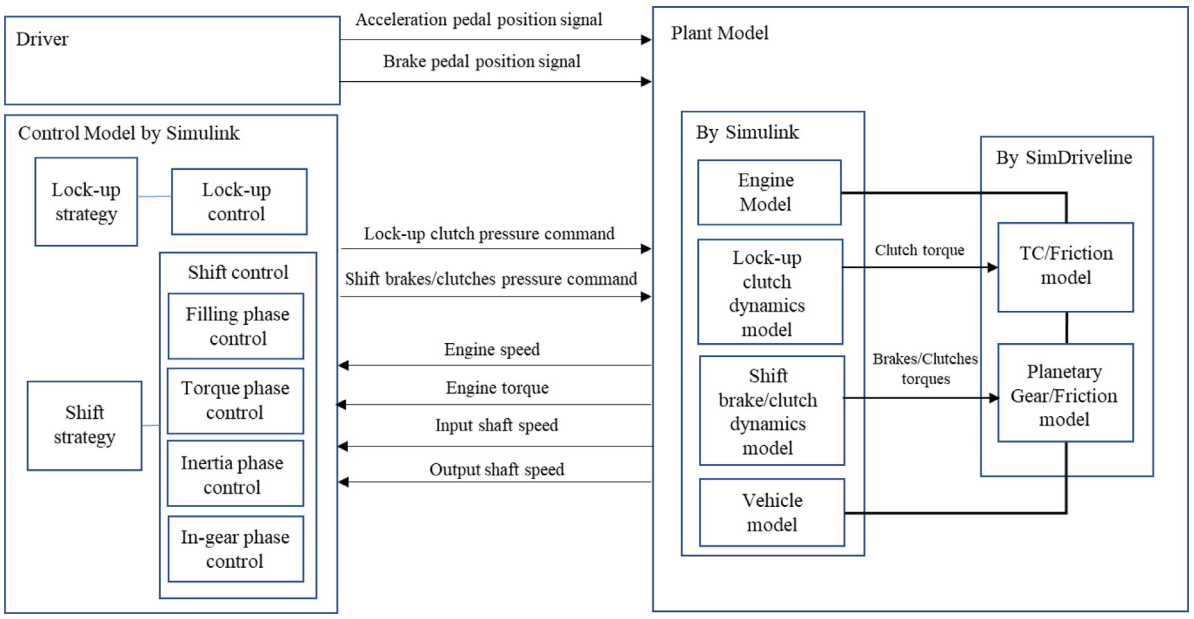

Fig. 6. Simulation model structure.

2.5. Closed clutch torque calculation

There is a problem in calculating clutch torque with hyperbolic model: if a clutch is closed, since the slip speed is zero, the model yields zero clutch torque. In this transmission specifically, C1 clutch is closed during 1st to 4th gear and C2 clutch is closed during 4th to 6th gear. Such problem can be resolved by changing that closed torque from right side (known variable) to left side (unknown variable) from Eqs. (22) and (23) in a similar way of reference [36]. Now, the new matrix can be formed as in Eqs. (30) and (31)

$$\mathrm{M}'\Omega' = B'T', \tag{30}$$

$$\Omega' = M'^{-1}B'T'. \tag{31}$$

Eqs. (32) and (33) shows the changed matrix, where a = −1, b = 0, c = 0, d = 1, x = c1, and y = c2 during 1st to 4th gear and a = 0, b = −1, c = 1, d = 0, x = c2, and y = c1 during 4th to 6th gear.

$$M' = \begin{bmatrix}
I_{s1} & 0 & 0 & 0 & 0 & 0 & 0 & 0 & 0 & 0 & S_1 & 0 & 0 & 0 & 0 & 1 & 0 & 0 & 0 \\
0 & I_{r1} & 0 & 0 & 0 & 0 & 0 & 0 & 0 & 0 & R_1 & 0 & 0 & -1 & 0 & 0 & 0 & 0 & 0 \\
0 & 0 & I_{c1} & 0 & 0 & 0 & 0 & 0 & 0 & 0 & -(S_1+R_1) & 0 & 0 & 0 & 0 & 0 & 0 & 1 & 0 \\
0 & 0 & 0 & I_{s2} & 0 & 0 & 0 & 0 & 0 & 0 & 0 & S_2 & 0 & 0 & 0 & -1 & 0 & 0 & a \\
0 & 0 & 0 & 0 & I_{r2} & 0 & 0 & 0 & 0 & 0 & 0 & R_2 & 0 & 0 & -1 & 0 & 0 & 0 & 0 \\
0 & 0 & 0 & 0 & 0 & I_{c2} & 0 & 0 & 0 & 0 & -(S_2+R_2) & 0 & 1 & 0 & 0 & 0 & 0 & 0 & b \\
0 & 0 & 0 & 0 & 0 & 0 & I_{s3} & 0 & 0 & 0 & 0 & 0 & S_3 & 0 & 0 & 0 & 1 & 0 & 0 \\
0 & 0 & 0 & 0 & 0 & 0 & 0 & I_{r3} & 0 & 0 & 0 & 0 & R_3 & 0 & 0 & 0 & 0 & 0 & 0 \\
0 & 0 & 0 & 0 & 0 & 0 & 0 & 0 & I_{c3} & 0 & 0 & 0 & -(S_3+R_3) & 0 & 1 & 0 & 0 & 0 & 0 \\
0 & 0 & 0 & 0 & 0 & 0 & 0 & 0 & 0 & I_i & 0 & 0 & 0 & 0 & 0 & 0 & -1 & 0 & 1 \\
0 & 0 & 0 & 0 & 0 & 0 & 0 & 0 & 0 & 0 & I_o & 0 & 0 & 0 & 0 & 0 & 0 & -1 & 0 \\
S_1 & R_1 & -(S_1+R_1) & 0 & 0 & 0 & 0 & 0 & 0 & 0 & 0 & 0 & 0 & 0 & 0 & 0 & 0 & 0 & 0 \\
0 & 0 & 0 & S_2 & R_2 & -(S_2+R_2) & 0 & 0 & 0 & 0 & 0 & 0 & 0 & 0 & 0 & 0 & 0 & 0 & 0 \\
0 & 0 & 0 & 0 & 0 & 0 & S_3 & R_3 & -(S_3+R_3) & 0 & 0 & 0 & 0 & 0 & 0 & 0 & 0 & 0 & 0 \\
0 & -1 & 0 & 0 & 0 & 1 & 0 & 0 & 0 & 0 & 0 & 0 & 0 & 0 & 0 & 0 & 0 & 0 & 0 \\
0 & 0 & 0 & 0 & -1 & 0 & 0 & 0 & 1 & 0 & 0 & 0 & 0 & 0 & 0 & 0 & 0 & 0 & 0 \\
1 & 0 & 0 & -1 & 0 & 0 & 0 & 0 & 0 & 0 & 0 & 0 & 0 & 0 & 0 & 0 & 0 & 0 & 0 \\
0 & 0 & 0 & 0 & 0 & 0 & 1 & 0 & 0 & -1 & 0 & 0 & 0 & 0 & 0 & 0 & 0 & 0 & 0 \\
0 & 0 & 1 & 0 & 0 & 0 & 0 & 0 & 0 & 0 & -1 & 0 & 0 & 0 & 0 & 0 & 0 & 0 & 0 \\
0 & 0 & 0 & a & 0 & b & 0 & 0 & 0 & 1 & 0 & 0 & 0 & 0 & 0 & 0 & 0 & 0 & 0
\end{bmatrix},$$

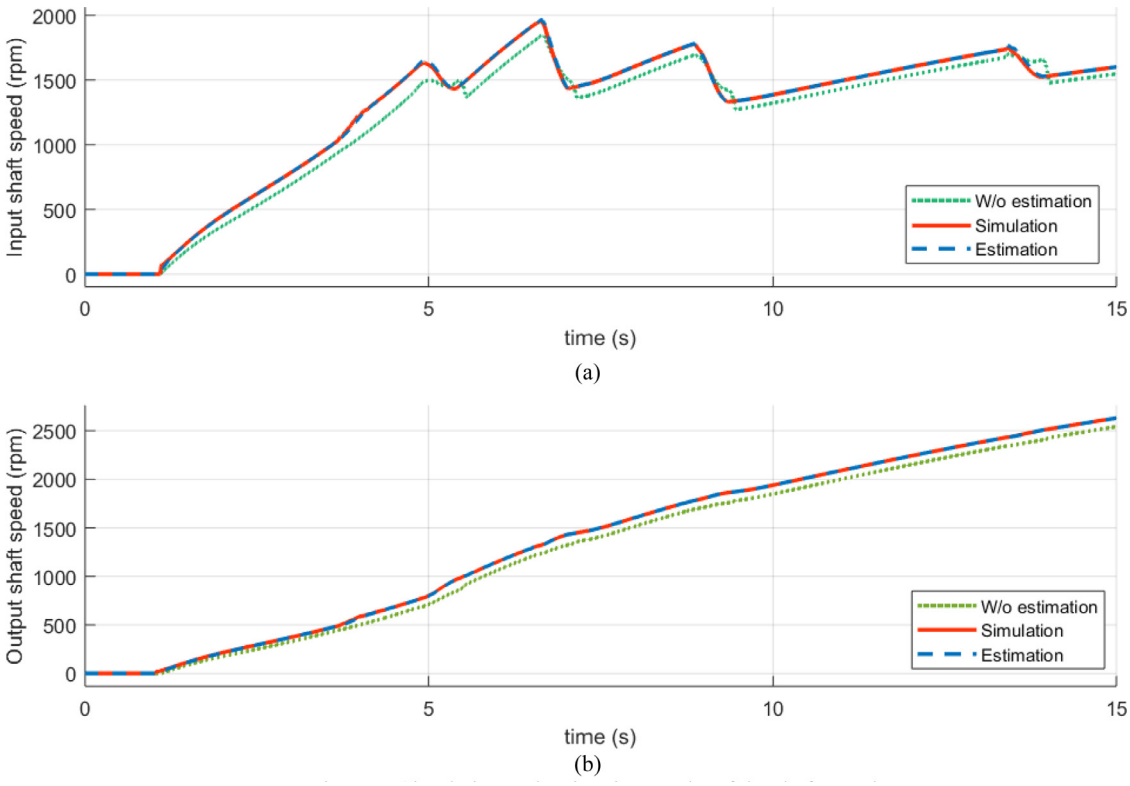

Fig. 7. Simulation and estimation results of the shaft speed.

$$\Omega' = \begin{bmatrix} \dot{\omega}_{s1} \\ \dot{\omega}_{r1} \\ \dot{\omega}_{c1} \\ \dot{\omega}_{s2} \\ \dot{\omega}_{r2} \\ \dot{\omega}_{c2} \\ \dot{\omega}_{s3} \\ \dot{\omega}_{r3} \\ \dot{\omega}_{c3} \\ \dot{\omega}_{i} \\ \dot{\omega}_{o} \\ F_1 \\ F_2 \\ F_3 \\ F_4 \\ F_5 \\ F_6 \\ F_7 \\ T_o \\ T_x \end{bmatrix}, \tag{32}$$

$$B' = \begin{bmatrix} 0 & 0 & 0 & 0 & 0 & 0 \\ 1 & 0 & 0 & 0 & 0 & 0 \\ 0 & 0 & 0 & 0 & 0 & 0 \\ 0 & 0 & 0 & c & 0 & 0 \\ 0 & 1 & 0 & 0 & 0 & 0 \\ 0 & 0 & 0 & d & 0 & 0 \\ 0 & 0 & 0 & 0 & 0 & 0 \\ 0 & 0 & 1 & 0 & 0 & 0 \\ 0 & 0 & 0 & 0 & 0 & 0 \\ 0 & 0 & 0 & -1 & 1 & 0 \\ 0 & 0 & 0 & 0 & 0 & -1 \\ 0 & 0 & 0 & 0 & 0 & 0 \\ 0 & 0 & 0 & 0 & 0 & 0 \\ 0 & 0 & 0 & 0 & 0 & 0 \\ 0 & 0 & 0 & 0 & 0 & 0 \\ 0 & 0 & 0 & 0 & 0 & 0 \\ 0 & 0 & 0 & 0 & 0 & 0 \\ 0 & 0 & 0 & 0 & 0 & 0 \\ 0 & 0 & 0 & 0 & 0 & 0 \\ 0 & 0 & 0 & 0 & 0 & 0 \end{bmatrix}, \quad T' = \begin{bmatrix} T_{B1} \\ T_{B2} \\ T_{B3} \\ T_y \\ T_i \\ R_r \end{bmatrix}. \tag{33}$$

2.6. Output shaft torque estimation

Input and output shaft speed equation from Eqs. (31)–(33) can be expressed by Eqs. (34) and (35). The coefficients $a_{10,1} \ldots a_{11,6}$ of Eqs. (34) and (35) are elements of matrix of $M'^{-1}B'$. The subscript of each coefficient states row and column of that matrix. Input and output shaft speed estimation can be built in a form of Luenberger observer as shown by Eqs. (36) and (37) using the input and output shaft speed measurements

$$\dot{\omega}_i = a_{10,1}T_{B1} + a_{10,2}T_{B2} + a_{10,3}T_{B3} + a_{10,4}T_y + \ a_{10,5}T_i + \mathrm{a}_{10,6}\mathrm{R_r}, \tag{34}$$

$$\dot{\omega}_o = a_{11,1}T_{B1} + a_{11,2}T_{B2} + a_{11,3}T_{B3} + a_{11,4}T_y + a_{11,5}T_i + a_{11,6}R_r, \tag{35}$$

$$\dot{\hat{\omega}}_i = a_{10,1}T_{B1} + a_{10,2}T_{B2} + a_{10,3}T_{B3} + a_{10,4}T_y + a_{10,5}T_i + a_{10,6}R_r + L_1\left(\omega_i - \hat{\omega}_i\right), \tag{36}$$

$$\dot{\hat{\omega}}_o = a_{11,1}T_{B1} + a_{11,2}T_{B2} + a_{11,3}T_{B3} + a_{11,4}T_y + a_{11,5}T_i + a_{11,6}R_r + L_2\left(\omega_o - \hat{\omega}_o\right). \tag{37}$$

From above equations, $a_{l,\,m}$ is row l and column m component of matrix $M'^{-1}B'$.

Eq. (38) shows the output shaft torque reformulated from Eq. (3). It is also dependent on output shaft acceleration and output shaft torque estimation also can be built using output shaft speed observer gain as shown in Eq. (39). It shows that even if there is some modeling error in Rr, such error can be compensated from speed difference between the estimated and measured value.

$$T_o = I_o\dot{\omega}_o + R_r, \tag{38}$$

$$\hat{T}_o = I_o\dot{\hat{\omega}}_o + R_r = I_o\dot{\omega}_o + R_rI_oL_2\left(\omega_o - \hat{\omega}_o\right). \tag{39}$$

2.7. Brake/clutch parameter adaptation

Since modeling of the brake/clutch parameters are variable according to temperature, duration time and wear, they should be adapted. Note that the number of adaptation variables has been decreased to four from five by comparing Eqs. (33) to (23). This is possible because those parameters adaptation is not necessary for already closed clutch. From Eqs. (34) to (35), the total number of unknown parameters is four but it can be decreased to two. This is because the remaining two brake and clutch torques are always zero during the gear shift. If the number of measurements is two, at most, two unknown parameters can be always adapted without fulfilling the PE (persistence of excitation) condition [32,37]. For example, during 1st to 2nd gear shift, input and output shaft acceleration is only the function of the B1 brake and the B2 brake torques as shown in Eqs. (40) and (41). This is because the B3 brake and the C2 clutch torques are zeros from Table 1.

$$\dot{x}_1 = \dot{\omega}_{in} = a_{10,1}T_{B1} + a_{10,2}T_{B2} \ + a_{10,5}T_i + a_{10,6}R_r, \tag{40}$$

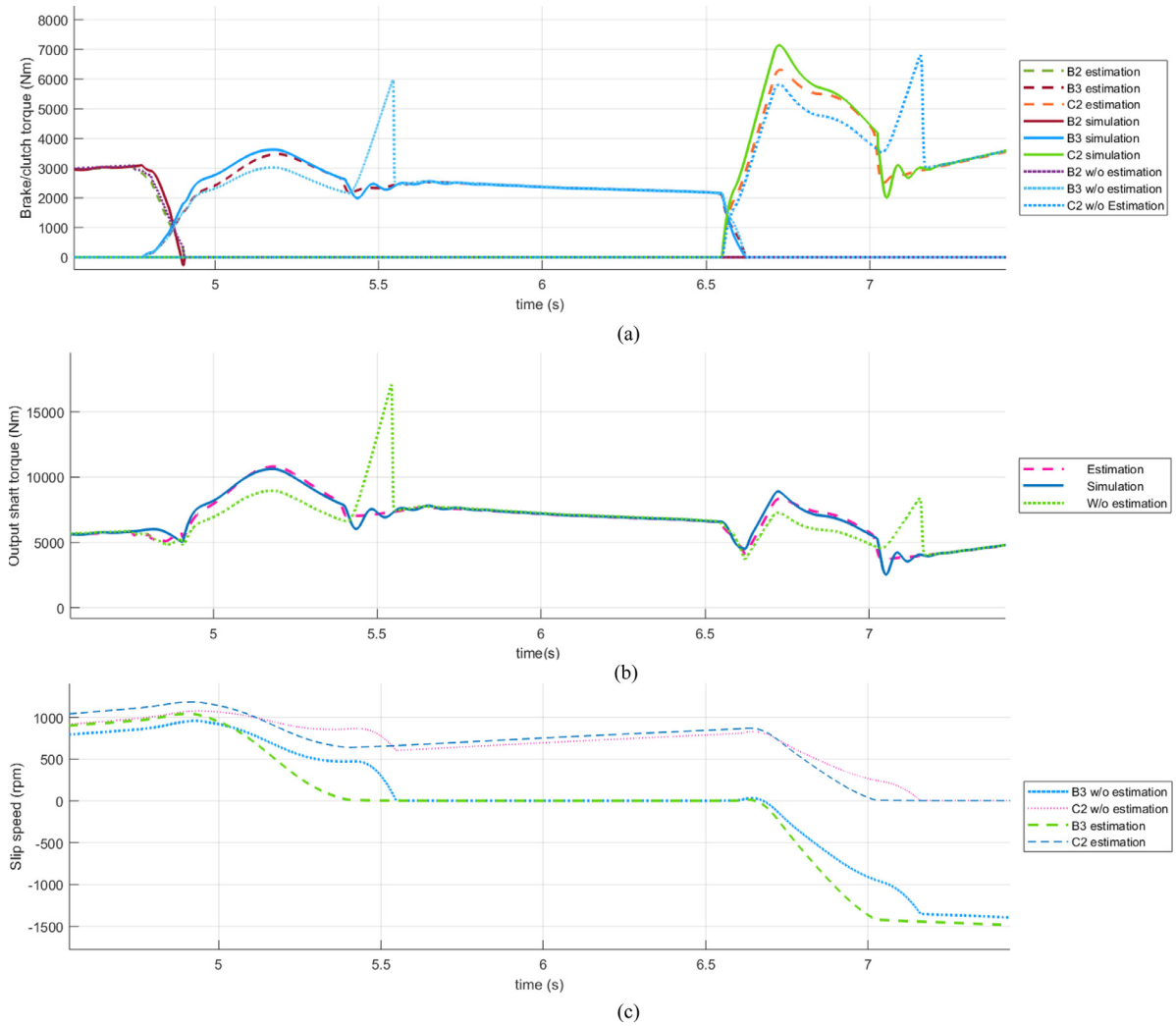

Fig. 8. Estimated transmission torque and speed (2nd to 3rd and 3rd to 4th gear shifts).

$$\dot{x}_2 = \dot{\omega}_{out} = a_{11,1}T_{B1} + a_{11,2}T_{B2} + a_{11,5}T_i + a_{11,6}R_r. \tag{41}$$

The brake torque Eq. (25) can be expressed to Eq. (42) in which the friction coefficient is separated into known part and unknown part.

$$T_B = \mu nr(AP - k(y_i + y))\tanh(\Delta\omega/\alpha) = (\mu_k + \mu_u)N, \tag{42}$$

where μ_k, μ_u mean nominal friction coefficient, unknown friction coefficient and N is as an Eq. (43).

$$N = nr(AP - k(y_i + y))\tanh(\Delta\omega/\alpha). \tag{43}$$

It has also unknown part due to the variation of stiffness k according to temperature and duration time, and incorrect position y_i according to brake/clutch wear. Therefore, Eq. (42) can be derived to Eq. (44)

$$T_B = (\mu_k + \mu_u)(N_k + N_u) = \mu_k N_k + \mu_k N_u + \mu_u N_k + \mu_u N_u = \mu_k N_k + \varepsilon, \tag{44}$$

where $\varepsilon = \mu_k N_u + \mu_u N_k + \mu_u N_u$. Therefore, T_B can be formed as an Eq. (45).

$$T_B = (\mu_k + \varepsilon/N_k)N_k = (\mu_k + \tau)N_k, \tag{45}$$

Where $\tau = \varepsilon/N_k$. Note that τ looks like the only unknown friction coefficient but it also includes the unknown part of N. Therefore, the B1 and the B2 brake torque can be formed as in Eqs. (46) and (47) where τ_{B1} and τ_{B2} are assumed to be slowly varying.

$$T_{B1} = \left(\mu_{B1,k} + \tau_{B1}\right)N_{B1,k}, \quad \dot{\tau}_{B1} \approx 0, \tag{46}$$

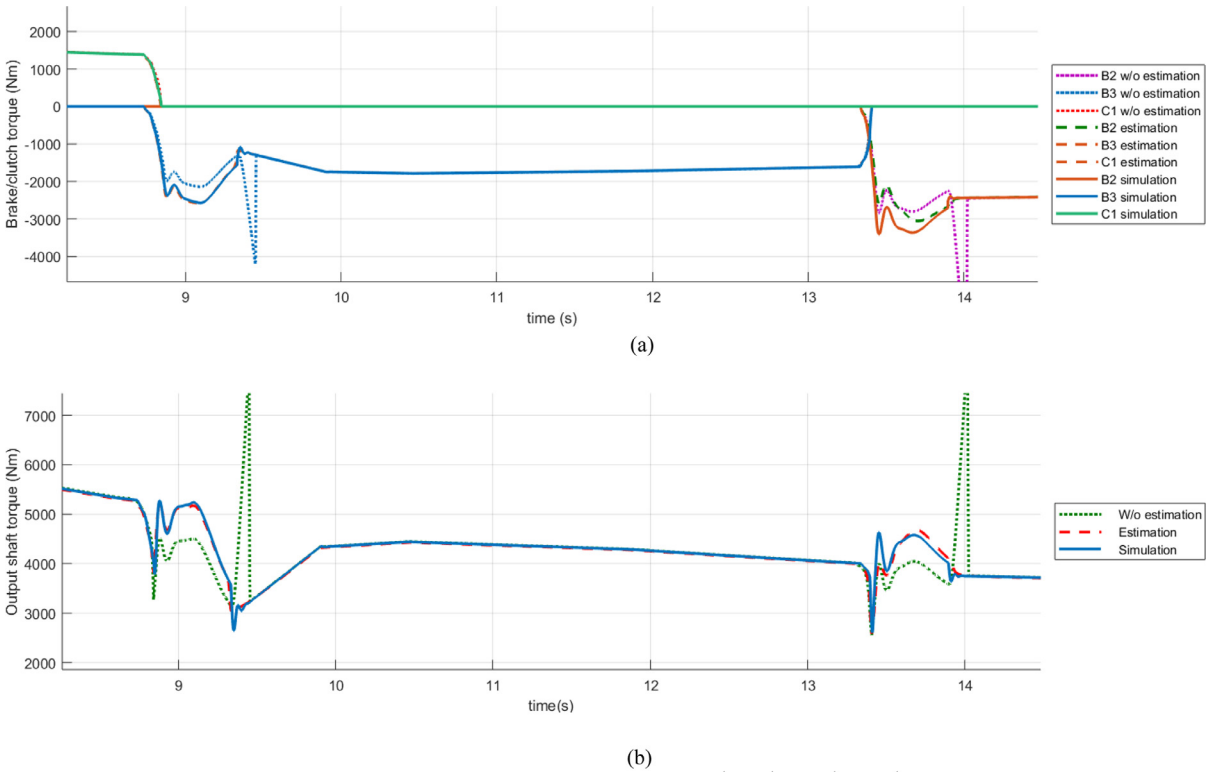

Fig. 9. Estimated transmission torque and speed (4th to 5th and 5th and 6th gear shifts).

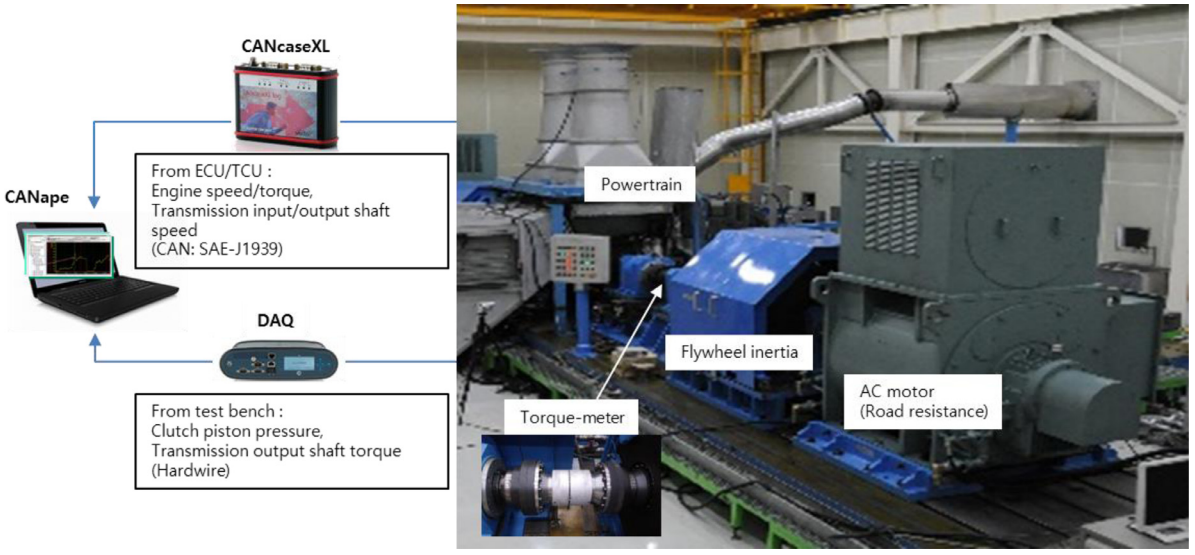

Fig. 10. Test bench environment.

$$T_{B2} = \left(\mu_{B2,k} + \tau_{B2}\right) N_{B2,k},\ \dot{\tau}_{B2} \approx 0. \tag{47}$$

Considering that temperature and wear effects are slowly progressing, it is reasonable to assume that τ_{B1} and τ_{B2} are slowly varying. On the other hand, in the case of friction coefficient variation, since brake/clutch slip speed rapidly varies, it can be cleared using the test data of friction coefficient on the brake and clutch slip speed.

The estimator can be set up as shown in Eqs. (48) and (49).

$$\dot{\hat{x}}_1 = a_{10,1}\hat{T}_{B1} + a_{10,2}\hat{T}_{B2} + a_{10,5}T_i + a_{10,6}R_r + L_1\tilde{x}_1, \tag{48}$$

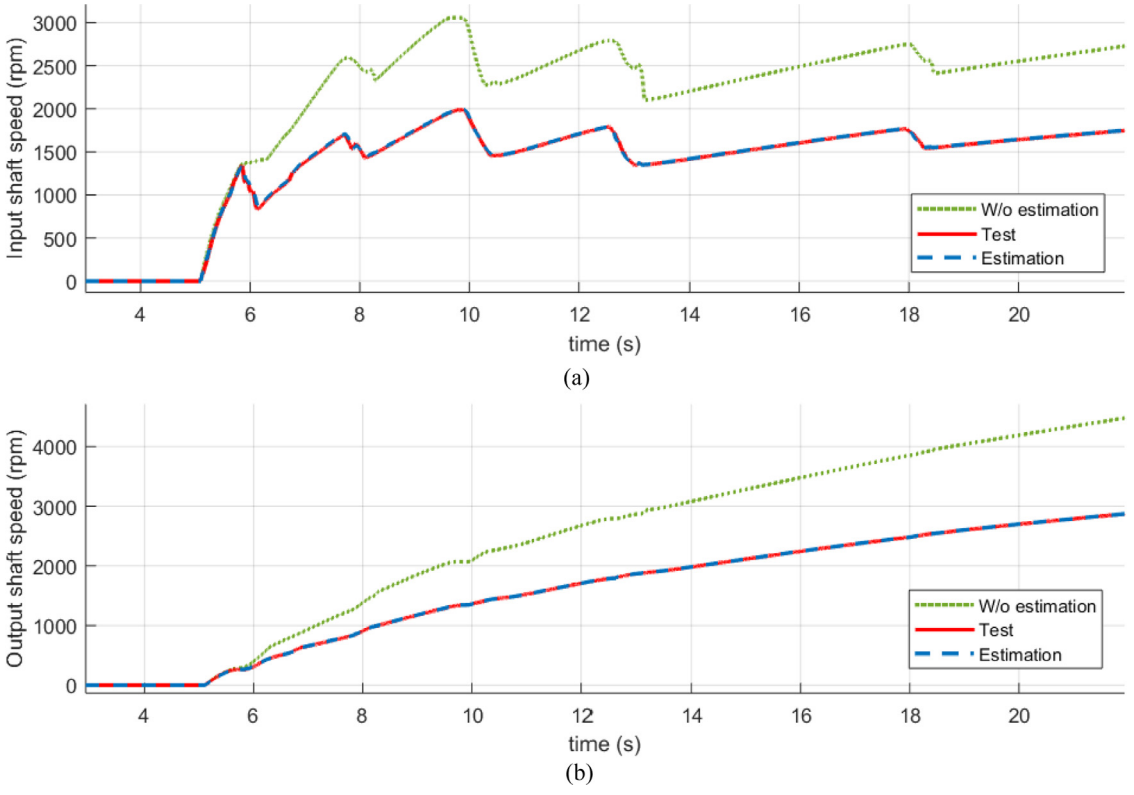

Fig. 11. Test and estimation results of the shaft speed.

$$\dot{\tilde{x}}_2 = a_{11,1}\hat{T}_{B1} + a_{11,2}\hat{T}_{B2} + a_{11,5}T_i + a_{11,6}R_r + L_2\tilde{x}_2. \tag{49}$$

Adaptation law and a Lyapunov function candidate are expressed as Eqs. (50)–(52).

$$\dot{\hat{\tau}}_{B1} = \gamma_1(a_{10,1}\tilde{x}_1 + a_{11,1}\tilde{x}_2)N_{B1,k}, \tag{50}$$

$$\dot{\hat{\tau}}_{B2} = \gamma_2(a_{10,2}\tilde{x}_1 + a_{11,2}\tilde{x}_2)N_{B2,k}, \tag{51}$$

$$V = \frac{1}{2}\tilde{x}_1^2 + \frac{1}{2}\tilde{x}_2^2 + \frac{1}{2\gamma_1}\tilde{\tau}_{B1}^2 + \frac{1}{2\gamma_2}\tilde{\tau}_{B2}^2. \tag{52}$$

Time differentiation of V can be expressed in Eq. (53) because $\dot{\tilde{\tau}}_{B1} = \dot{\tau}_{B1} - \dot{\hat{\tau}}_{B1} \approx \dot{\tilde{\tau}}_{B1}$.

$$\begin{aligned}\dot{V} &= \tilde{x}_1\dot{\tilde{x}}_1 + \tilde{x}_2\dot{\tilde{x}}_2 + \frac{1}{\gamma_1}\tilde{\tau}_{B1}\dot{\tilde{\tau}}_{B1} + \frac{1}{\gamma_2}\tilde{\tau}_{B2}\dot{\tilde{\tau}}_{B2} \\ &= \tilde{x}_1\left(a_{10,1}\tilde{T}_{B1} + a_{10,2}\tilde{T}_{B2} - L_1\tilde{x}_1\right) + \tilde{x}_2\left(a_{11,1}\tilde{T}_{B1} + a_{11,2}\tilde{T}_{B2} - L_2\tilde{x}_2\right) - \frac{1}{\gamma_1}\tilde{\tau}_{B1}\dot{\hat{\tau}}_{B1} - \frac{1}{\gamma_2}\tilde{\tau}_{B2}\dot{\hat{\tau}}_{B2}\end{aligned} \tag{53}$$

Eq. (53) can be rearranged to Eq. (54) by substituting the Eqs. (46) and (47).

$$\dot{V} = \tilde{\tau}_{B1}\left((a_{10,1}\tilde{x}_1 + a_{11,1}\tilde{x}_2)N_{B1} - \frac{1}{\gamma_1}\dot{\hat{\tau}}_{B1}\right) + \tilde{\tau}_{B2}\left((a_{10,2}\tilde{x}_1 + a_{11,2}\tilde{x}_2)N_{B2} - \frac{1}{\gamma_2}\dot{\hat{\tau}}_{B2}\right) - L_1\tilde{x}_1^2 - L_2\tilde{x}_2^2. \tag{54}$$

It can be simplified to Eq. (55) by substituting the Eqs. (50) and (51) if the adaptation gains are chosen as $L_1, L_2 > 0$

$$\dot{V} = -L_1\tilde{x}_1^2 - L_2\tilde{x}_2^2 \le 0. \tag{55}$$

In order to demonstrate the asymptotic stability of the estimator, it is necessary to consider following set:

$$\Omega = \{\ \tilde{x}_1,\ \tilde{x}_2,\ \tilde{\tau}_{B1}, \tilde{\tau}_{B2} |\ \tilde{x}_1,\ \tilde{x}_2 = 0\}, \tag{56}$$

where $V = 0$.

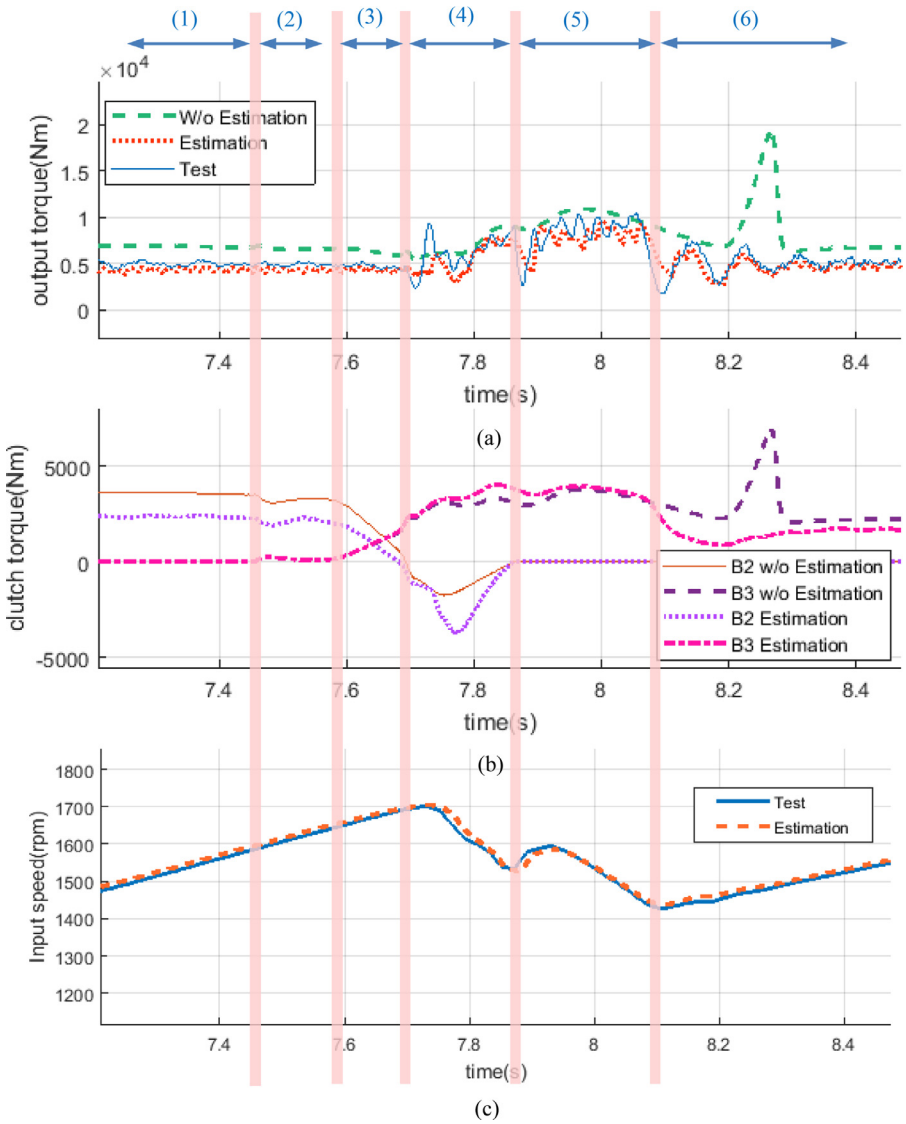

Fig. 12. Estimated torque (2nd to 3rd shift.

If the$\tilde{x}_1, \tilde{x}_2 = 0$, then $\dot{\tilde{\tau}}_{B1} \approx -\dot{\hat{\tau}}_{B1} = 0$ and $\dot{\tilde{\tau}}_{B2} \approx -\dot{\hat{\tau}}_{B2} = 0$ by Eqs. (48) and (49). Therefore $\tilde{x}_1,\ \tilde{x}_2,\ \tilde{\tau}_{B1}, \tilde{\tau}_{B2}=0$ is the only invariant subset of (56) and the estimation errors asymptotically converge to zero [37].

Adaptation gains $\gamma_1,\ \gamma_2$ which determine the adaptation rates can be tunable. They are, also, related to L_1, L_2, which are Luenberger observer gains. If the L_1, L_2 were selected to high, $\tilde{x}_1,\ \tilde{x}_2$ become small; thus $\dot{\hat{\tau}}_{B1}, \dot{\hat{\tau}}_{B2}$ became small from Eqs. (50) and (51). Therefore, adapted values can't follow actual ones even though $\gamma_1,\ \gamma_2$ are high enough.

The final estimator structure is schematically illustrated in Fig. 5.

3. Verification by simulation

3.1. Controller and plant modeling for simulation

The estimator performance is tested with the gear shift scenario via simulation. Fig. 6 shows the simulation model structure. Basic transmission control model is constituted by Simulink. The lock-up and shift strategy decide when the lock-up engages and gear shift happens according to the engine speed, input shaft speed, and output shaft speed. The lock-up and shift control builds the pressure command of the lock-up and shift brakes and clutches. Shift control is divided by four phases. The kiss point pressures are commanded in filling phase. Feed forward torque control is working on torque phase

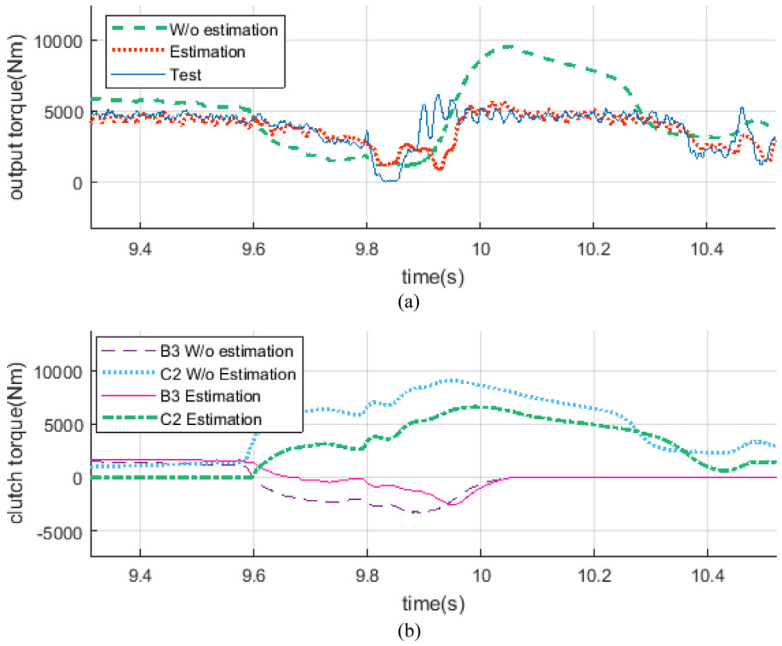

Fig. 13. Estimated torque (3rd to 4th shift).

and feed forward torque control and feedback target input speed control is working on inertia phase. The maximum pressures are commanded in-gear phase. They will be discussed more specifically during the test result analysis in chapter 4.

Plant Model is composed of equations using Simulink and SimDriveline. Simulink model is composed of Engine, lock-up and shift, brake and clutch dynamics, and longitudinal vehicle load resistance. Planetary gear, torque converter, and brake and clutch friction is simulated by a widely used driveline simulation tool SimDriveline. In fact, as the friction model in SimDriveline precisely describes the realistic friction behavior, it is reasonable to compare the estimated clutch torques with simulated torques.

All of the coefficients in equations (1) ∼ (12) and (25) ∼ (28) are set to be same to those of estimator without the output shaft inertia in Eq. (3) and the friction coefficients in Eqs. (25) and (27). The output shaft inertia, which includes vehicle inertia from the estimator, is set to be 5% larger than that of plant model in order to make the different acceleration, which can check up the effectiveness of the estimation logic. In addition, the known friction coefficients from the estimator in Eqs. (44) and (45) are set to 0.10 while those of plant model are set to 0.12. Such different setting will make the different brake/clutch torques and is suitable in checking the effectiveness of the adaptation logic.

The simulation includes a typical power-on upshift during acceleration from 2nd to 6th gear shifts with 100% acceleration pedal position. Initially, vehicle launches with torque converter mode at 2nd gear and lock-up clutch engages during 2nd gear. Thus, the transmission gear shift is performed with lock-up mode for the whole 2nd to 6th gear shifts.

3.2. Speed estimation

Fig. 7 shows comparison results of Lagrange model with and without proposed estimation. The proposed estimation method shows superior estimating performance without signal lagging.

3.3. Torque estimation

Fig. 8 shows simulation results of 2nd to 3rd and 3rd to 4th gear shifts and Fig. 9 shows that of 4th to 5th and 5th to 6th gear shifts. In Fig. 8(a) and (b), during no-shift area the brake, clutch and output shaft torque of the proposed estimation and Lagrange model show similar results comparing to that of simulation. However, during the shift area, estimation result follows the simulation result extraordinarily comparing to that of Lagrange model.

One notable observation in the simulation result of brake, clutch, and output shaft torque is the immediate torque increase at the end of each shift. Such immense torque increase occurs due to the absence of an estimator which exactly compensates clutch/brake slip condition. In fact, such result is the typical characteristics of the clutch model. When transmission controller detects speeds synchronization from constantly comparing output speed and input speed with target gear ratio, control input enables maximum clutch pressure increase in order to prevent clutch slip. Clutch model operates as the clutch torque follows to clutch torque capacity when the clutch status is slipping; and it follows to engaged torque when the clutch status is engaged. In Fig. 8(c), the brake slip speed by Lagrange model is still quite high. Thus, brake torque follows

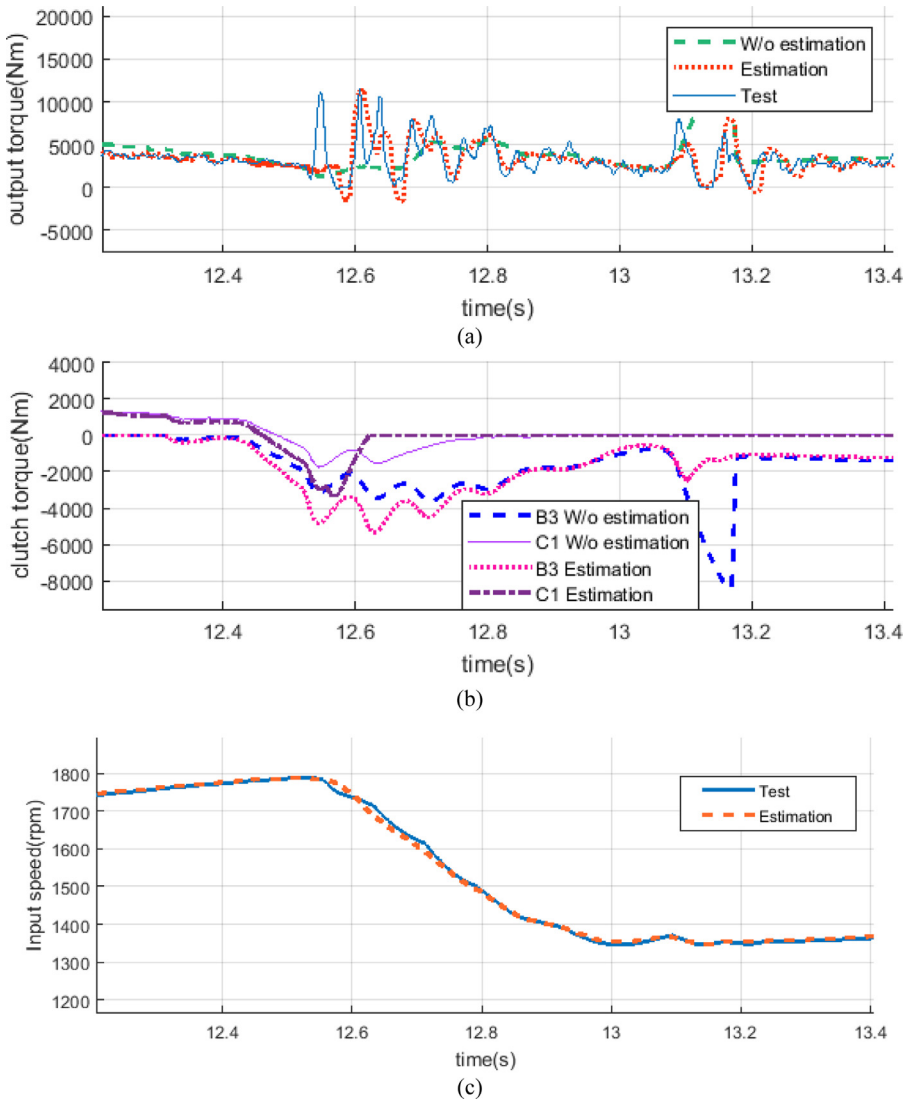

Fig. 14. Estimated torque (4th to 5th shift).

brake torque capacity and converges to engaged torque as the slip speed decreased to near zero. On the other hand, slip speed by proposed estimator decreases to near zero at the end of shift which enables high torque estimation performance for engaged torque. All the brakes or clutches and output torque of the other shift show similar tendencies.

Off-going brake and clutch follows the simulation result well. Although the on-coming clutch torque shows differences at the start of shift since the nominal friction coefficient is assumed to be lower than that of the model value, the clutch torque converges to the simulation result as shift progresses by the adaptation logic. This result shows effectiveness of the logic. It follows the simulation result well after the late inertia phase, because in this simulation, friction coefficient is assumed to be constant. This is clear if the test results of friction coefficient on the brake and clutch slip speed are used instead of constant coefficient as it was discussed before.

The negative torque means the change of torque direction. In case of 4th to 5th gear shift, on-coming brake (the B3 brake) estimation follows the simulation result well from the initial point because the B3 brake friction coefficient is already adapted during the 2nd to 3rd gear shift.

4. Verification by experiment

In order to show the applicability of the proposed estimator for the production transmissions, it is tested on the actual transmission. A transmission dynamometer test bench is used for the test. Fig. 10 shows the test bench environment. Equivalent flywheel inertia is set up between the transmission output shaft and the AC motor in order to consider the vehicle

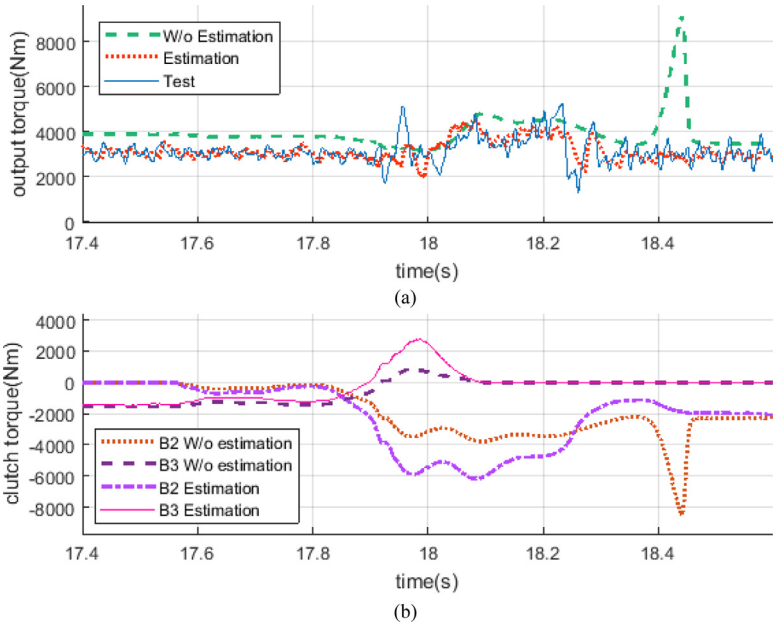

Fig. 15. Estimated torque (5th to 6th shift).

inertia. The AC motor controls the road resistance. A Torque-meter, which can measure the output shaft torque, is installed between the transmission output shaft and the flywheel inertia. The data acquisition system synchronizes both the TCU data by the CAN protocol and the dynamometer data by hardwire.

The test scenarios include 1st to 6th gear shift during full torque acceleration mode. The validation of the proposed estimator is conducted by comparing the estimated output torque to the measured output torque. This is due to the absence of brake or clutch sensors on the real production transmission. However, the former simulation results showed that the estimation performance is effective as the comparison result between the output torque estimator and measured output torque shows satisfactory correlations.

4.1. Speed estimation

Fig. 11 shows the input and output shaft speeds of Lagrange model with and without estimation. The transmission is operated in torque converter mode during 1st gear and at the initial time of 2nd gear (until 7.5 s). Input speed and output speed of the Lagrange model without estimation can't track the test result whereas estimation result with adaptation shows good correlation.

4.2. Torque estimation

Fig. 12 shows the output torque, brake torques, and input speed during 2nd to 3rd gear shift. Fig. 12(a) shows tracking performance of output torque estimation to the measured value. In Fig. 12(b), torque estimation shows the big negative torque, which means that the off-going brake disengagement is too late. It would make big inter-lock of input shaft speed which can be seen in Fig. 12(c).

The clutch torque state can be descripted in detail by six phases. Phase (1) is the 2nd gear-engaged phase. Phase (2) is the filling phase where transmission oil fills in the piston of on-coming clutch for kiss-point torque whereas off-going torque decreases until the clutch torque capacity. Phase (3) is the torque phase where on-coming clutch increases the torque and off-going clutch decreases the torque, resulting in torque transfer.

Phase (4) is the inter-lock phase. In the initial point this phase, theoretically, when torque transfer is completed and resulting off-going torque became zero, piston oil should be drained completely; however, in the real situation, it is extremely difficult to search the exact point where off-going clutch torque reaches zero. Such difficulty may be due to several factors including transmission modelling error or poor control algorithm. Thus, remaining pressure causes negative clutch torque, resulting in inter-lock or power circulation inside the transmission. Due to the inter-lock in the transmission, the input shaft speed slightly falls for speed adjustment. On the other hand, when off-going clutch pressure drops too early, input speed flare can occur.

For good shift quality, it is optimal for torque phase to be continuously connected to inertia phase without inter-lock or flare. Phase (5) is the inertia phase where on-coming clutch torque control and input speed deceleration occur. Finally, Phase

(6) is the 3rd gear-engaged phase where on-coming clutch is engaged completely, resulting in torque decrease to engaged torque.

Fig. 13 shows enlarged view of the output torque, brake, and clutch torques during 3rd to 4th gear shift. Note that in Fig. 13(a), there exist immense discrepancy between the torque by Lagrange model and measured torque. Such huge differences in torque is mainly because on-coming (C2) clutch torque from Lagrange model possesses an offset (about 1,300 Nm) where measured pressure is zero. This is due to the accumulating computation error in slip speeds and rotating oil speed within the clutch, resulting in wrong calculation of centrifugal pressure, which yields torque offset.

Such argument can be backed up from the observation in Fig. 13(b) result; the remaining centrifugal pressure causes the torque offset which is not desirable in the beginning phase of the shift. On the other hand, the torque from the proposed estimation shows the zero on-coming clutch torque at the beginning of the shift, which is highly desirable for exceptional shifting quality.

Fig. 14 shows the brake and clutch torques, output torque and input speed during 4th to 5th gear shift. Estimated torque follows the measured torque value well while torque by Lagrange model shows poor tracking performance to the measured torque as shown in Fig. 14(a). The Fig. 14(b) shows the off-going (C1) clutch torque by Lagrange model that the C1 clutch disengaged at 12.80 s. However, the estimated torque result shows that the clutch disengaged at 12.62 s. This means inertia phase starts earlier comparing to that of Lagrange model. In Fig. 14(c), input speed decreases at 12.58 s which is the starting point of inertia phase. Therefore, it is safe to conclude that the estimator result is more reasonable than that of the Lagrange model.

Fig. 15 shows the brake torques and output torque during 5th to 6th gear shift. Estimated torque follows the measured value well while there is a big discrepancy between torque by Lagrange model and measured torque as shown in Fig. 15(a). Fig. 15(b) shows that there is much more on-coming engaging torque and off-going interlock torque than those of the Lagrange model.

5. Conclusion

Due to the needs of fuel economy and fast response of the vehicle, many ATs select clutch-to-clutch control in lock-up mode. Therefore, the shift quality becomes an exceptionally critical factor where torque-based control is a suitable choice. In this study, dynamic drive torque estimation for any types of ATs was investigated which is applicable to torque control or torque monitoring practically. The proposed estimation method is established based on the whole gear shift model. It also exploits the clutch model which requires no switching between the models during the clutch slip and engagement. Therefore, it makes continuous estimation possible during the whole shift. In addition, building the specific brake and clutch models separately according to their own characteristics increases their applicability to the real wet type AT. In fact, adaptive clutch torque estimator was developed to respond to the clutch parameter variation during the shift.

The proposed method estimated the brake and clutch torques and output shaft torque effectively from the simulation result despite of the presence of modeling error. Finally, from the experiment results, it estimated the output torque accurately in spite of the transmission modeling errors. Therefore, it is also concluded that the estimated clutch torque is accurate and well describes the typical clutch-to-clutch phenomena such as inter-locking.

References

[1] H. Wakamatsu, T. Ohashi, S. Asatsuke, Y. Saitou," Honda's 5 speed All Clutch to Clutch Automatic Transmission", SAE Technical Paper 2002-01-0932, 2002
[2] H. Tsutsui, T. Hisano, A. Suzuki, M. Hijikata, M. Taguchi, K. Kojima,"Electro-Hydraulic Control System for AISIN AW New 6-speed Automatic Transmission", SAE Technical Paper 2004-01-1638, 2004
[3] Y. Fu, Y. Liu, L. Cui, X. Xu, Dynmic analysis and control strategy of wet cltuches during torque phase of gear shift, J. Mech. Sci. Technol. 30 (2015) 1479–1496.
[4] B. Gao, H. Chen, K. Sanada, Two-degree-of freedom controller design for clutch slip control of automatic transmission, SAE Int. J. Passeng. Cars- Mech. Syst. 1 (2008) 430–438.
[5] D. Yanakiev, Y. Fujii, E. Tseng, G.M. Pietron, J.F. Kucharski, "Closed-loop torque phase control for shifting automatic transmission gear ratios based on friction element load estimation", US patent, No.8510003, 2013.
[6] M. Goetz, M. Levesley, D. Crolla, Dynamics and control of gearshifts on twin-clutch transmissions, Proc. Inst. Mech. Eng. Part D J. Automob. Eng. 219 (2005) 951–963.
[7] M. Kulkarni, T. Shim, Y. Zhang, Shift dynamics and control of dual-clutch transmissions, Mech. Mach. Theory 42 (2007) 168–182.
[8] P.D. Walker, N. Zhang, R. Tamba, Control of gear shifts in dual clutch transmission powertrains, Mech. Syst. Sig. Process. 25 (2011) 1923–1936.
[9] K. van Berkel, T. Hofman, A. Serrarens, M. Steinbuch, Fast and smooth clutch engagement control for dual-clutch transmissions, Control Eng. Pract. 22 (2014) 57–68.
[10] Y. Liu, D. Qin, H. Jiang, Y. Zhang, Shift control strategy and experimental validation for dry dual clutch transmissions, Mech. Mach. Theory 75 (2014) 41–53.
[11] S. Kim, J. Oh, S. Choi, Gear shift control of a dual-clutch transmission using optimal control allocation, Mech. Mach. Theory 113 (2017) 109–125.
[12] K.-s. Yi, B.-K. Shin, K.-I. Lee, Estimation of turbine torque of automatic transmissions using nonlinear observers, J. Dyn. Syst. Meas. Contr. 122 (2000) 276–283.
[13] J.-O. Hahn, K.-I. Lee, Nonlinear robust control of torque converter clutch slip system for passenger vehicles using advanced torque estimation algorithms, Veh. Syst. Dyn. 37 (2002) 175–192.
[14] B.K. Shin, J.O. Hahn, and K.I. Lee, "Development of shift control algorithm using estimated turbine torque," SAE Technical Paper 0148-7191, 2000.
[15] R.A. Masmoudi, J.K. Hedrick, Estimation of vehicle shaft torque using nonlinear observers, J. Dyn. Syst. Meas. Contr. 114 (1992) 394–400.
[16] S. Watechagit and K. Srinivasan, "Modeling and simulation of a shift hydraulic system for a stepped automatic transmission," SAE Technical Paper 0148-7191, 2003.

[17] M. Ibamoto, H. Kuroiwa, T. Minowa, K. Sato, and T. Tsuchiya, "Development of smooth shift control system with output torque estimation," SAE Technical Paper 0148-7191, 1995.
[18] B. Gao, H. Chen, Y. Ma, K. Sanada, Design of nonlinear shaft torque observer for trucks with Automated manual transmission, Mechatronics 21 (2011) 1034–1042.
[19] J. Kim, S.B. Choi, Control of dry clutch engagement for vehicle launches via a shaft torque observer, in: American Control Conference (ACC), 2010, pp. 676–681.
[20] Z.-G. Zhao, J.-L. Jiang, Z.-P. Yu, T. Zhang, Starting sliding mode variable structure that coordinates the control and real-time optimization of dry dual clutch transmissions, Int. J. Automot. Technol. 14 (2013) 875–888.
[21] M. Wu, J. Zhang, T. Lu, C. Ni, Research on optimal control for dry dual-clutch engagement during launch, Proc. Inst. Mech. Eng. Part D J. Automob. Eng. 224 (2010) 749–763.
[22] V. Tran, J. Lauber, M. Dambrine, Sliding mode control of a dual clutch during launch, in: The second international conference on engineering mechanics and automation (ICEMA2), 2012, pp. 16–17.
[23] Z. Bin, L. Tongli, H.Hongtao Z.Jianwu, Micro-slip control and torque estimation for dual clutch transmission, Proc. Inst. Mech. Eng. Part K J. Multi-body Dyn. 231 (2017) 750–764.
[24] Z. Zhao, X. Li, L. He, C. Wu, J.K. Hedrick, Estimation of torques transmitted by twin-clutch of dry dual clutch transmission during vehicle's launching process, IEEE Trans. Veh. Technol. (2016).
[25] F. Winchel, W. Route, in: Design practices: Passenger Car Automatic Transmission, vol.5, SAE, PA, 1988, pp. 79–105. ch. Ratio Changing the Passenger Car Automatic Transmission.
[26] Z. Zhao, L. He, Y. Yang, C. Wu, X. Li, J.K. Hedrick, Estimation of torque transmitted by clutch during shifting process for dry dual clutch transmission, Mech. Syst. Sig. Process. 75 (2016) 413–433.
[27] H. Hao, T. Lu, J. Zhang, Estimation of transmitted torques in dual-clutch transmission systems, Insight-Non-Destr. Test. Cond. Monit. 57 (2015) 464–471.
[28] J. Wu, P.D. Walker, J. Ruan, N. Zhang, Target torque estimation for gearshift in dual clutch transmision with uncertain parameters, Appl. Math. Model. vol. 51 (2017) 1–20.
[29] R. Losero, J. Lauber, T.-M. Guerra, P. Maurel, Dual clutch torque estimation based on an angular discrete domain Takagi-Sugeno switched observer, in: Fuzzy Systems (FUZZ-IEEE), 2016 IEEE International Conference on, 2016, pp. 2357–2363.
[30] J.J. Oh, S.B. Choi, J. Kim, Driveline modeling and estimation of individual clutch torque during gear shifts for dual clutch transmission, Mechatronics 24 (2014) 449–463.
[31] J.J. Oh, S.B. Choi, Real-time estimation of transmitted torque on each clutch for ground vehicles with dual clutch transmission, Mechatron. IEEE/ASME Trans. 20 (2015) 24–36.
[32] S. Kim, J. Oh, S. Choi, Driveline Torque Estimations for a Ground Vehicle with Dual-Clutch Transmission, IEEE Trans. Veh. Technol. 67 (2018) 1977–1989.
[33] S. Kim, J. Oh, S. Choi, Control-oriented Modelling and Torque Estimations for Vehicle Driveline with Dual-clutch Transmission, Mech. Mach. Theory 121 (2018) 633–649.
[34] K.D. Mishra, K. Srinivasan, Robus control and estimation of clutch-to-clutch shifts, Control Eng. Pract. 65 (2018) 100–114.
[35] S. Bai, J. Maguire, H. Peng, Dynamic Analysis and Control System Design of Automatic Transmissions, SAE international, Warrendale, 2013.
[36] S. Lee, Y. Zhang, D. Jung, A systematic approach for dynamic analysis of vehicles with eight or more speed automatic transmission, J. Dyn. Syst. Meas. Control 136 (2014) 5.
[37] P.A. Ioannou and J. Sun, Robust adaptive control: Courier Corporation, 2012.